Development of Environmental Contours for Ice Ridge Statistics Applied to Reliability-based Design of Arctic Ships

Wei Chai[1]*, Bernt J. Leira[1], Arvid Naess[2], Knut Vilhelm Høyland[3], Sören Ehlers[4]

[1] Department of Marine Technology, Norwegian University of Science and Technology

[2] Department of Mathematical Sciences, Norwegian University of Science and Technology

[3] Sustainable Arctic Marine and Coastal Technology (SAMCoT), Centre for Research-based Innovation (CRI), Norwegian University of Science and Technology

[4] Institute for Ship Structural Design and Analysis, Hamburg University of Technology

*corresponding author: chai.wei@ntnu.no

Abstract: Ice ridges are assumed to pose a major threat to ships and offshore structures in sea ice infested areas without icebergs, since they determine and govern the design loads of the structures. In this work, the concept of environmental contours is introduced for first-year ice ridge statistics to describe the collection of extreme ice ridge conditions, as well as for the estimation of extreme ice loads that act on ship structures. Probabilistic models are introduced to describe the key parameters of the first-year ice ridges that govern the ship and ice ridge interaction process. Based on the inverse first order reliability method (IFORM), the development of environmental contours used for the reliability-based design of ice-capable vessels in Arctic regions is studied. Different forms (dimensions) of environmental contours are generated according to different simplifications of the interaction process. Furthermore, the influence of the correlations between the environmental parameters and occurrence rate (or encounter frequency) for ice ridge and ship interaction processes on environmental contours are studied.

Keywords: environmental contours; ice ridge; Arctic ships; reliability-based design

1. Introduction

The reduction of the extent and thickness of ice in the Arctic in recent decades has resulted in increased demands for developing offshore structures to explore natural resources (such as oil, gas and minerals) and ice-capable vessels to navigate along Arctic shipping routes (Hahn et al., 2017). For ice-capable vessels sailing in Arctic regions, a number of different ice types will be encountered, such as level ice, broken ice, rafted ice, ice rubble fields and ice ridges.

The ice conditions along the Arctic shipping routes mostly consist of first-year ice, with few ice features appearing in the summer season. Among the aforementioned ice types, first-year sea ice ridges are assumed to pose a major threat to ships in Arctic regions since they determine and govern the design loads on the ship hull (ISO, 2010).

Current Arctic ship designs are mainly based on rules and regulations, such as the Finnish-Swedish Ice Class Rules (FSICR), International Association of Classification Societies (IACS) Polar Class rules, International Maritime Organization (IMO) Polar code, and so on. These rules for ship structural design primarily rely on experience and deterministic solutions (Ehlers et al., 2017) and are attractive due to the simplicity of their application. However, ice-induced loads on ship hulls are random by nature (Chai et al., 2018; Lensu, 2002). The randomness is caused by the variation of ice conditions (e.g., the physical and mechanical properties) in the Arctic regions and by the complexity of the ship and ice interaction process in association with various force components (Riska, 1987). Therefore, probabilistic methods should be applied to describe the stochastic aspects of ice loads, and a reliability-based design method that takes into consideration the randomness and uncertainties of the ice conditions and ice loads could enrich current rule-based design methods.

Within the framework of reliability-based design, the Ultimate Limit States (ULS) criteria which ensure that no significant structural damage occurs during the design life of a structure, is an essential requirement. For the design of Arctic ships, the ULS criteria mean that the vessel should be able to withstand the ice load actions associated with a specific exceedance probability (or a specific return period), both for the local and global actions of the vessels (Riska and Bridges, 2017). In this study, the local ice loads is considered, which refers to the loads induced by the ice features on the ship's shell structure and acting on the transvers frames in the bow region during the ship and ice ridge interaction process. Generally, the most appropriate and accurate approach to estimate extreme ice loads is the full long-term response analysis that accounts for the contribution from each ice condition with specific physical and mechanical parameters and the probability of occurrence of each specific ice condition. However, such a long-term analysis is usually time-consuming for numerical simulations with a high accuracy and expensive in regard to the required experiments (Leira, 2008).

In order to improve the efficiency of the ULS design at the early design stage, the environmental contour method is commonly applied as an alternative to the full long-term analysis. In this method, the environmental contour is defined as a collection of environmental conditions (first-year ice ridge conditions in this work) that correspond to a given return period

(DNV.GL, 2017). Then, the desired extreme ice loads for the same return period can be approximately estimated on the basis of ice loads from the worst ice conditions along the generated environmental contour. In this method, numerical simulations (or experiment) are only required for some selected ice conditions located on the environmental contour to calculate ice ridge loads and find the worst ice condition.

Traditionally, the environmental contour for a given return period is established by the inverse first order reliability method (IFORM) and the joint probabilistic distributions of the environmental parameters (Winterstein et al., 1993). In addition to the IFORM, there are other methods to generate environmental contours, such as Monte Carlo simulation (Huseby et al., 2013), the inverse second order reliability method (ISORM) (Chai and Leira, 2018), the principal component analysis method (Eckert-Gallup et al., 2016), and so on.

In this work, the concept of environmental contour is introduced for first-year ice ridge conditions, and the procedure of applying the environmental contour method to estimate extreme ice loads is illustrated. The main focus is the development of environmental contours for ice ridge statistics. Specifically, the key parameters of ice ridges, which determine the ice loads on ship hulls, are identified according to the mechanisms behind the ice ridge and ship interaction process, and then, probabilistic models are applied to describe these key parameters. On the basis of the IFORM and distributions of the key parameters for ice ridges, different dimensions of environmental contours for a given return period are generated according to different simplifications of the interaction process.

2. First-year sea ice ridge

2.1 Properties of ice ridges

Sea ice can be divided into first-year, second-year and multi-year ice. In the Arctic basin and surrounding seas, floating sea ice generally grows to a thickness of 1.0-2.5 m, reaching its maximum thickness in April-May. As the air temperature increases during the summer season, the ice thickness decreases during the melting process. If the sea ice survives one or more summers, it is called old ice, which has stronger mechanical properties than first-year sea ice. In this work, first-year ice conditions are considered. The physical and mechanical properties of first-year ice have been extensively studied, but very limited progress has been made regarding understanding old ice. Additionally, most of old ice exists at very high latitudes, and sea ice along Arctic Shipping routes is mostly first-year ice.

Figure 1. An Arctic ship sailing in an ice ridge field (Wikipedia, edited on May 4, 2018)

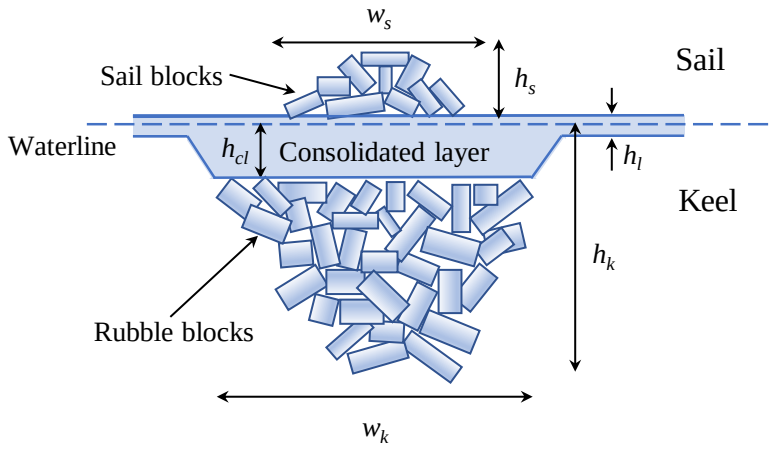

Figure 2. A first-year ice ridge with some key parameters: sail draft h_s, sail width w_s, level ice thickness h_l, consolidated layer thickness h_{cl}, keel draft h_k and keel width w_k (Strub-Klein and Sudom, 2012)

Among the various ice conditions along Arctic shipping routes, first-year ice ridges are regarded to be a major threat that should be considered during the design stage. A typical example for a ship in an ice ridge field is presented in Fig. 1. Basically, a ridge is a line or wall of broken sea ice features that are forced up by pressure or shear (Sanderson, 1988). When level ice floes are compressed and/or sheared by environmental driving forces, such as wind and current forces, ice ridges are formed as broken ice rubbles at the early stage. Then, these blocks can be consolidated to some extent by the refreezing process. As shown in Fig. 2, first-year sea ice ridges usually consist of three distinguishable parts (ISO, 2010): the sail, consolidated layer and rubble. The sail is the part that is above the water and has pores filled with air and snow. The underwater part is called the ridge keel and comprises the other two parts of the sea ice ridge. For the upper part of the keel, the consolidated layer is a continuous layer of ice due to

the refrozen ice blocks, while in the lower part of the keel, the ice blocks are loose and partially refrozen. These rubble blocks are packed together due to buoyancy forces with water trapped between the blocks. Additionally, some key parameters for the geometry of a first-year sea ice ridge are marked and illustrated in Fig. 2.

2.2 A review of ship and ice ridge interaction

Previous studies of ship and ice ridge interactions are limited due to the complexity of the interaction process. Basically, there are three methods that can be applied to predict the ice ridge loads that act on structures, i.e., analytical (or semi-analytical) methods, numerical simulations and experiments (Høyland, 2014). In analytical methods, the ship and ice ridge interaction model is very simple and with easy calculations. For example, in Sudom and Timco (2013), the effects from the sail part of the first-year ice ridge can be neglected since the volume of the sail is small compared to that of the keel part. Ice ridge forces for ship-shaped structures can be divided into loads components from the consolidated layer and forces from the rubble blocks. The thickness of the consolidated layer can reach 2.0-2.5 times the surrounding level ice thickness and the mechanical properties of the consolidated layer are assumed to be close to that of the surrounding level ice. Therefore, the consolidated layer is considered to be a thick level ice and the ice load components can be estimated by using the relevant empirical formula recommended in the ISO standard and other rules. Moreover, to estimate the load component generated by the rubble blocks, there is another empirical formula based on the passive failure model suggested by the ISO standard. However, this model is mainly used for fixed structures and there is no previous application for ships.

For the numerical simulation, the consolidated layer and rubble blocks are usually modelled as a solid material (i.e., thick level ice) and granular materials, respectively. Various studies have been performed to numerically assess the ship and level ice interaction, such as a three degree-of-freedom rigid model developed by Su et al. (2010), which is applied to simulate the hull-ice interaction and ship maneuvers in level ice. Later, this model was extended to six degrees-of-freedom by Tan et al. (2013). Additionally, some numerical methods, such as the finite element method (FEM), GPU (graphics processing unit) computation basis (Hahn et al., 2017; Huisman et al., 2016), cohesive element method (Lu et al., 2014) and finite-discrete element method (FEM-DEM) (Ranta et al., 2018) have been developed to study the interactions between level ice and ship/slope structures. Numerical methods, such as the DEM (Gong et al., 2017) and FEM (Sand and Horrigmoe, 2001) have also been applied to study the ice rubbles

interaction with the ship and slope structure, respectively. However, due to the complexity of ice ridges and the ship interaction process, there has been no work on numerical simulation of the ship and ice ridge keel interaction with simultaneous considerations of the effects from the two different parts of the ridge keel.

Scale model tests and field tests of ship and ice ridge interactions can enrich our understanding for the ridge breaking process, even though relevant studies are very limited. For example, at the Hamburg Ship Model Basin (HSVA), model tests were performed to study the interaction process between ships and ice ridges (Myland, 2014). In this study, both the ridge sail and keel (with the consolidated layer part and ice rubbles) were considered. A ship can break through sea ice ridges either continuously or by ramming, which depends on the ridge breaking energy, propulsive energy and kinetic energy of the vessel. Additionally, model tests performed at HSVA for a moored slope structure have confirmed the common knowledge that ice loads due to ice ridges are significantly higher than loads caused by the surrounding level ice (Dalane et al., 2015). Furthermore, field experiments performed on ships (or slope structures) interacting with first-year ice ridges have been reported in Kujula (1994), Lemee and Brown (2005) and Kuuliala et al. (2017), etc.

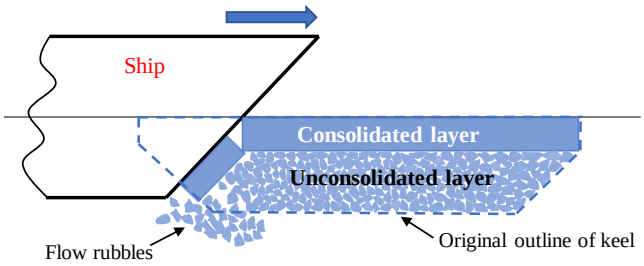

Figure 3. Illustration of a ship interacting with a typical first-year ice ridge

Based on previous studies of first-year ice ridges interacting with ships and slope structures, the ship-ice ridge interaction process is illustrated in Figure 3. The local ice loads acting on the ship bow region is considered in this study. During the preliminary design stage, the effect of the ridge sail part can be neglected, ice loads from the ridge keel can be divided into two parts, i.e., the components due to the consolidated layer part and loads caused by unconsolidated ice rubbles. The consolidated layer is assumed to be thick level ice. Generally, the ship-level ice interaction process is initiated by a localized crushing of the ice edge, and then, the contact area between the ship and ice sheet as well as the crushing force increase with the ship advancing and penetrating the ice features. The ice sheet eventually deflects and the bending stresses

promote a flexural failure at a certain breaking distance from the interaction region. The block rubbles can be broken through by the ship structure with kinetic energy and propulsive energy, as well as by the broken consolidated layer part. Furthermore, flow rubbles and broken blocks detached from the keel part of the ridge can be cleared by the local water current.

3. Environmental contour method for reliability-based design

In this section, the principle of the environmental contour method used for reliability-based design and the generation of the environmental contour based on the IFORM are introduced. The ULS criteria is expressed in the following form:

$$G(y_c, \mathbf{S}) = y_c - Y(\mathbf{S}) \tag{1}$$

where $G(\cdot)$ denotes the failure function and the n-dimensional vector $\boldsymbol{S} = (S_1, S_2, \ldots, S_n)^{\mathrm{T}}$ represents the environmental variables with the joint probability density function (PDF), $f_{\boldsymbol{S}}(\boldsymbol{s})$. $Y(\boldsymbol{S})$ is the loads acting on the structure and y_c is the deterministic design capacity of the structure.

The failure probability p_f for the structure can be calculated as follows:

$$p_f(y_c) = \int_{G(y_c,\mathbf{S})\le 0} f_{\mathbf{S}}(\mathbf{s})d\mathbf{s} \tag{2}$$

The integrals given in Eq. 2 can be solved exactly when the joint PDF and failure function $G(y_c, \boldsymbol{S})$ are given. However, such cases are rare in reality and the value of $Y(\boldsymbol{S})$ in the failure function for a specific environmental condition $(s_1, s_2, \ldots, s_n)^{\mathrm{T}}$ is usually obtained from a numerical simulation or experiment. The integrals can also be approximated by applying a Monte Carlo simulation (MCS) or by the FORM and second order reliability method (SORM) (Madsen et al., 2006). For example, in the FORM, the integral and failure surface $G(y_c, \boldsymbol{S})$ are transformed into a space consisting of independent, standard Gaussian variables (i.e. the U-space). The transformed failure surface is approximated by a tangent plane at the design point and then the failure probability is given as follows:

$$p_f(y_c) \approx \Phi(-\beta) \tag{3}$$

where Φ denotes the cumulative density distribution function (CDF) of the standard normal random variables, β is the reliability index and also the distance between the origin to the design point in the U-space.

However, determination of the design capacity, y_N, which can withstand the loads associated with a N-year return period (i.e., the load level is exceeded only once over the N-year period)

requires repeated calculations by changing the values of y_c. The failure function given by Eq. 1 will also change according to the values of y_c. Therefore, relevant iterations or interpolation schemes are required for the calculation procedure to determine the value of y_N.

In addition to the aforementioned methods for estimating the extreme load level (or design capacity), y_N, the environmental contour method is another approximation method. In this method, one assumes that the failure probability, $p_f(y_N)$ is given at first and then explores what types of restrictions are imposed on the environmental variables (Vanem, 2017). This restriction is given in the form of an environmental contour, which is a collection of environmental parameters associated with the same return period as the extreme load level. In this method, time-consuming numerical simulations or (expensive) experiments are required only for limited environmental conditions located on the environmental contour. Subsequently, the maximum loads for these selected conditions on the environmental contour can be applied to estimate the extreme load level, y_N, corresponding to the same return period (Haver and Winterstein, 2009; Winterstein et al., 1993).

Traditionally, the environmental contour for the N-year return period is derived in connection with the inverse FORM. As previously mentioned, the failure probability, $p_f(y_N)$, is given at first to generate the environmental contour that corresponds to the same return period. In the IFORM, a n-dimensional sphere with the radius β_F (given as Eq. 4) is initially created in the U-space.

$$\beta_F = \Phi^{-1}(1 - p_f(y_N)) \tag{4}$$

Then, the sphere in the U space is mapped into the physical parameter space as the environmental contour. Such a transformation is executed by applying the inverse Rosenblatt transformation if the joint distribution of the environmental parameters is described by the conditional modelling approach (Rosenblatt, 1952) or by the Nataf transformation if only the marginal PDFs of the environmental parameters and correlation coefficients of the environmental parameters are given (Silva-González et al., 2013). From this point, it is seen that the environmental contour obtained by the IFORM is a collection of environmental parameters (or conditions) in the physical parameter space corresponding to the parameters located on the sphere with a radius β_F in the U space.

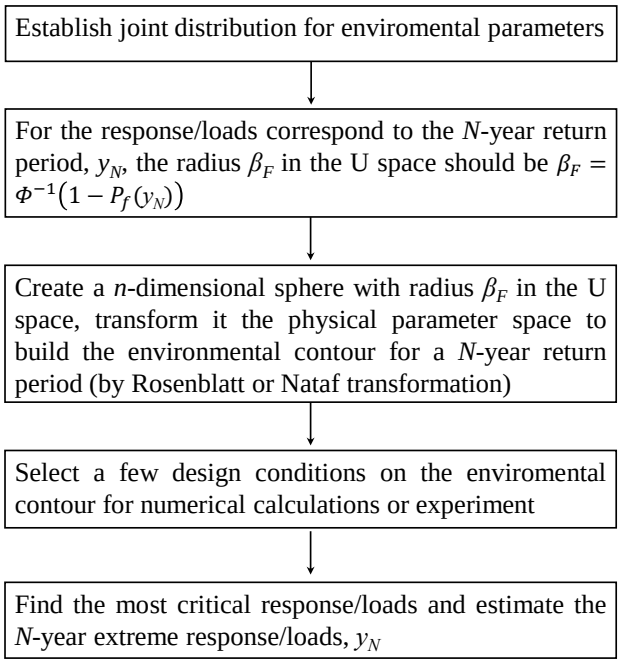

Figure 4. Flowchart of the environmental contour method used to estimate the extreme load level, y_N, associated with a N-year return period

Based on the aforementioned description, the main steps of the environmental contour method (ECM) for estimating extreme response/loads are illustrated in Fig. 4. The main advantage of the environmental contour method lies in the fact that the description of the environmental parameters is uncoupled from the structure response obtained from the numerical simulation or experiments. Due to its high efficiency and satisfactory accuracy, the environmental contour method has been widely applied for the ULS-based design at the early stage. Additionally, in this work, we assume that the ice ridge loads for a given ice ridge condition is a deterministic process. The most critical response, calculated by numerical simulation or obtained by experiment, for the environmental conditions located on the environmental contour can be used to estimate the N-year extreme loads. However, if the response process for a give condition is stochastic, the extreme response can be estimated by using a fractile, which is at a level higher than the median value of the extreme distribution, for the specific most serious environmental condition (DNV.GL, 2017).

4. Statistical models for key parameters

Based on the descriptions of the ship and first-year ice ridge interaction process provided in Section 2.2, four variables of the first-year ice ridge are selected as the key parameters for establishing the environmental contours that are used for reliability-based design. These key

parameters are the consolidated layer thickness, flexural and crushing strengths of the consolidated layer part and keel draft. As the first step of the flowchart shown in Fig. 4, statistical models should be applied to describe the aforementioned key parameters.

The consolidated layer thickness is believed to be dependent on met-ocean conditions. The thickness can be measured by mechanical or thermal drilling. In this work, the consolidated layer thickness of the ice ridges located in the Barents Sea are selected for study. The data sets of the consolidated layer thickness were collected by field measurements conducted by UNIS (University Centre in Svalbard) from 2002 to 2011. By applying a statistical analysis, it is found that the Gamma distribution provides a satisfactory description of the collected consolidated layer thickness. The Gamma distribution is expressed as follows:

$$f(h_{cl}) = \frac{1}{\Gamma(k)\theta^k} h_{cl}^{k-1} \exp(-\frac{h_{cl}}{\theta}) \tag{5}$$

where Γ is the gamma function, k and θ are the shape and scale parameters for the gamma distribution, respectively. Based on the experimental data, these two values are determined by applying the method of moments to be 2.97 and 0.54. The satisfactory fitting results of the Gamma distribution for the consolidated layer thickness are shown in Figs. 5 and 6 as a Q-Q plot and PDFs, respectively.

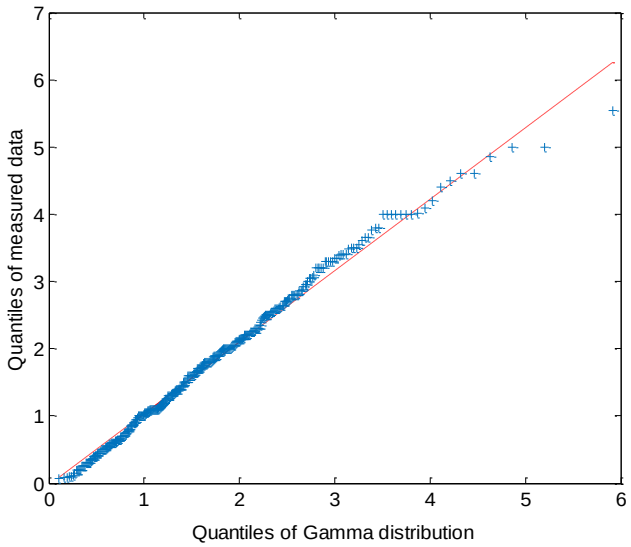

Figure 5. Q-Q plot for the gamma distribution applied to the consolidated layer thickness h_{cl}

It should be noted that, for different sea areas along the Arctic routes, the distribution of the consolidated layer thickness varies. In the Barents Sea, the measured data obtained by mechanical or thermal drilling are sufficient, but for the other sea areas with limited measured

or published data, the distribution of the consolidated layer thickness can be estimated by applying the data of the surrounding level ice thickness. Moreover, for some distributions where a probability paper fitting is not available, the Q-Q plot can provide a good and simple method to qualify the fitting between the data distribution and a hypothesized theoretical distribution.

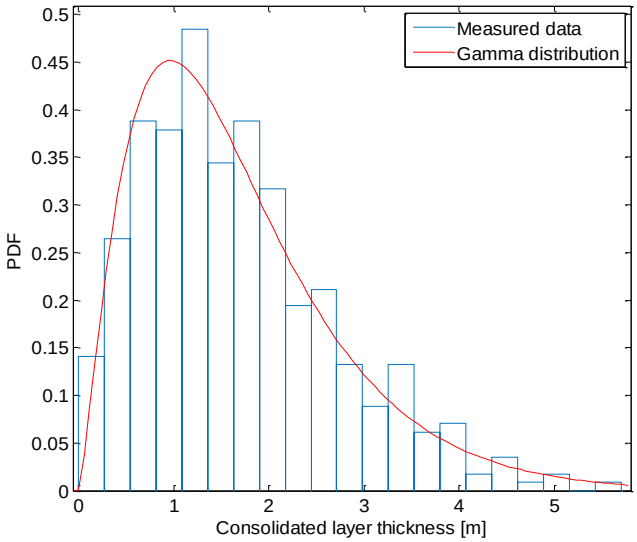

Figure 6. Probability density function for the consolidated layer thickness h_{cl}

The mechanical properties of the consolidated layer, such as the flexural strength and the crushing strength are assumed to be similar to those of the surrounding level ice due to the limited experimental data for the consolidated part of the ice ridge. There have been a large number of researchers who have measured the flexural strength of first-year sea ice in different Arctic regions (Timco and Weeks, 2010). Basically, the flexural strength of the sea ice depends on the average temperature, salinity and brine volume. In this work, the flexural strength data is collected from Timco and O'Brien (1994), which covers in situ experiment data from different regions, such as the Canadian and Alaskan Beaufort Sea, Baffin Island, Greenland and Gulf of Bothnia, etc. Statistical analysis demonstrates that the two-parameter Weibull distribution, given by Eq. 6, can be applied to describe the marginal PDF of the flexural strength.

$$f(\sigma_f) = \frac{\beta}{\alpha}\left(\sigma_f/\alpha\right)^{\beta-1} \exp\left(-\left(\sigma_f/\alpha\right)^{\beta}\right) \tag{6}$$

where σ_f is the flexural strength. The scale parameter α = 0.582 and shape parameter β = 2.090 are obtained from the probability paper method. The satisfactory fitting results for the flexural strength of first-year sea ice in the Arctic regions are shown in Figs. 7 and 8 as a Weibull probability paper plot and PDFs, respectively.

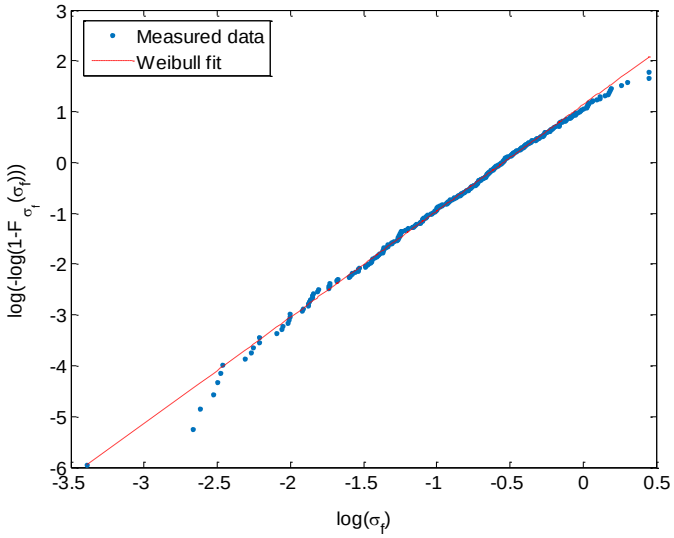

Figure 7. Weibull probability paper plot for the flexural strength of first-year level ice σ_f

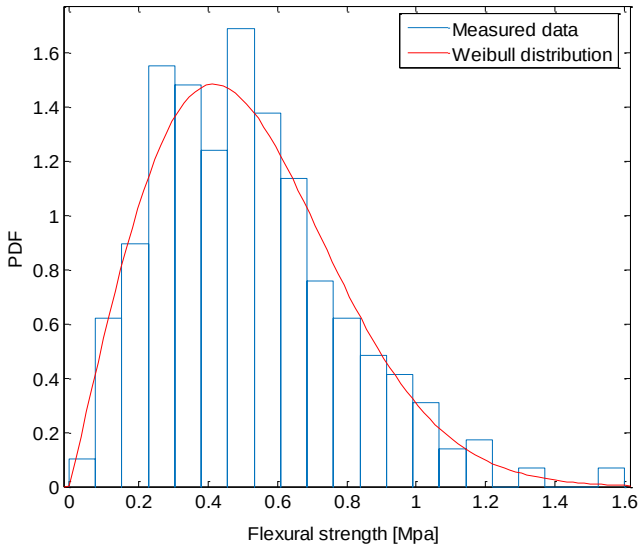

Figure 8. Probability density function for the flexural strength of first-year level ice σ_f

The crushing strength of level ice is dependent on the loading direction, porosity, salinity, temperature, failure mode, and so on. Since this work focuses on the topic of the ship and ice ridge interaction, the horizontally loaded samples should be considered. Although it has been reported in Timco and Weeks (2010) that many investigators have measured the compressive strength of first-year sea ice, published data for horizontally loaded samples in Arctic regions are very limited, except the in situ experiment data from the Svalbard regions and Barents sea. In recent years, Norwegian and Swedish research institutes have been continuously performing research work and field experiments in the Barents Sea. Based on the field experiment performed in the winter seasons from 2005-2012 (Bonath et al., 2013; Strub-Klein, 2017), 363 samples in total with horizontal loading were collected to study the stochastic properties of the crushing strength. For these samples, the stain rates are kept as a fixed value 10^{-3}/s during the

experiments. From the statistical analysis, it has been found that the lognormal distribution, given by Eq. 7, can provide a good description of the measured data.

$$f(\sigma_c) = \frac{1}{\sqrt{2\pi}\sigma \cdot \sigma_c} \exp\left(-\frac{(\ln \sigma_c - \mu)^2}{2\sigma^2}\right) \tag{7}$$

where σ_c denotes the crushing strength, $\mu = 0.644$ and $\sigma = 0.550$ are the mean value and standard deviation of the logarithmic values, respectively.

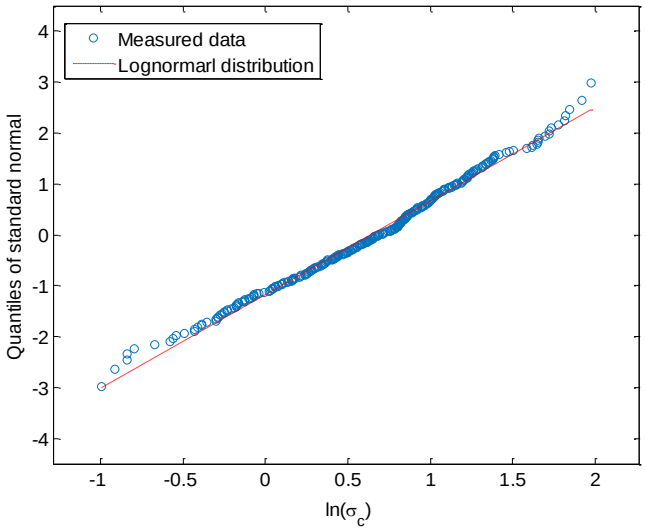

Figure 9. Standard Gaussian probability paper for the lognormal distribution applied to the crushing strength of first-year sea ice σ_c

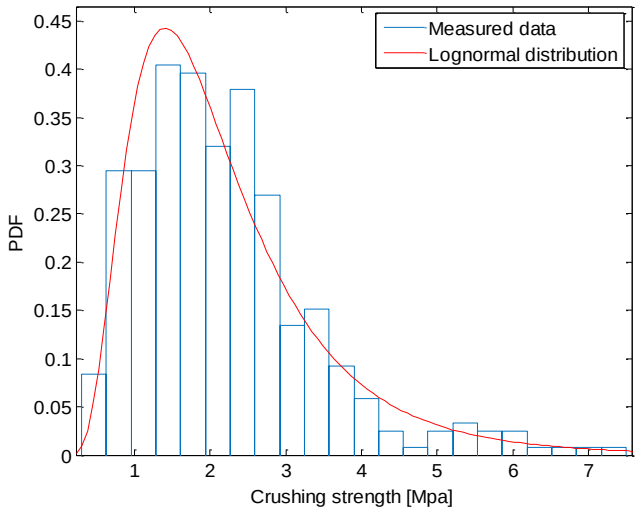

Figure 10. Probability density function of the crushing strength of first-year level ice σ_c

The fitting results of the lognormal distribution for the measured data are presented in Figs. 9 and 10 as a standard Gaussian probability paper plot and PDFs, respectively. It should be

noted that the current probabilistic model for the crushing strength is based on the measured samples from the Barents Sea and Svalbard regions.

The ice ridge loads on the ship structure from the rubble blocks are dependent on the keel draft, keel width, keel porosity and mass of the keel part. Among these parameters, the keel draft, h_k is the most important characteristic and depends on the met-ocean environment, including season variations as the consolidated layer thickness. For the other parameters, the ISO standard and Ref. (Strub-Klein and Sudom, 2012) provide some recommendations and suggestions for the relationships between different geometric parameters that can be used for the subsequent analysis.

The keel draft can be observed by drilling or by the continuous scanning method, such as the use of upward looking sonars which are either moored to the seabed or mounted on submarines. In this study, keel draft data for first-year ice ridges in different Arctic regions such as the Beaufort Sea, Greenland Sea, Barents Sea are selected for statistical analysis. These data sets are mainly collected by mechanical drilling and thermal drilling and were published in Strub-Klein and Sudom (2012). For the keel draft data collected in a specific sea area, it is found that the exponential distribution given by Eq. 8 can give a satisfactory description of the data (Wadhams, 1980).

$$f(h_k) = \lambda \exp(-\lambda(h_k - c)) \tag{8}$$

where h_k denotes the keel draft, λ is the shape factor of the distribution and the fixed value c can be regarded as the cut-off height.

However, when data are obtained from different sea ice areas, the authors found that the three-parameter Weill distribution given by Eq. 9 can provide a better description of the collected data than the exponential distribution which is a specific form of the three-parameter distribution (i.e., $\alpha = 1/\lambda$, β=1.0).

$$f(h_k) = \frac{\beta}{\alpha}\left(\frac{h_k - c}{\alpha}\right)^{\beta-1} \exp\left(-\left(\frac{h_k - c}{\alpha}\right)^{\beta}\right) \tag{9}$$

where the scale parameter α = 9.464, shape parameter β = 1.697 and location parameter c = 0.450 are obtained by the method of moments. The satisfactory fitting results are shown in Figs. 11 and 12 as a Weibull probability paper plot and PDFs, respectively.

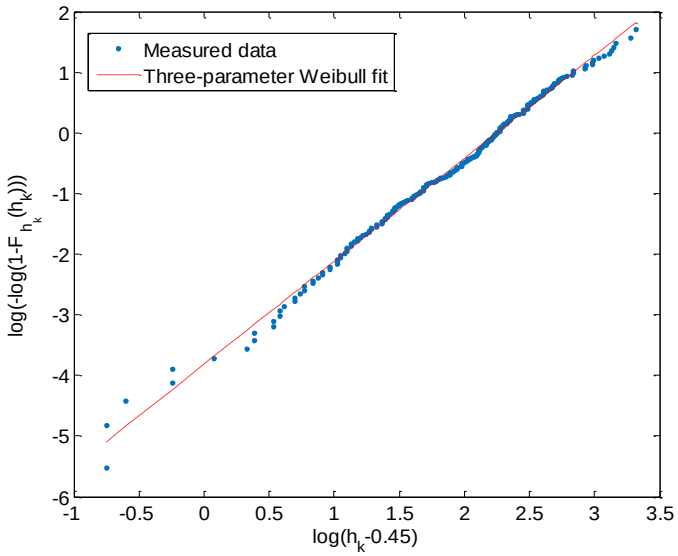

Figure 11. Three-parameter Weibull probability paper plot for the keel draft h_k of first-year ice ridges in Arctic regions

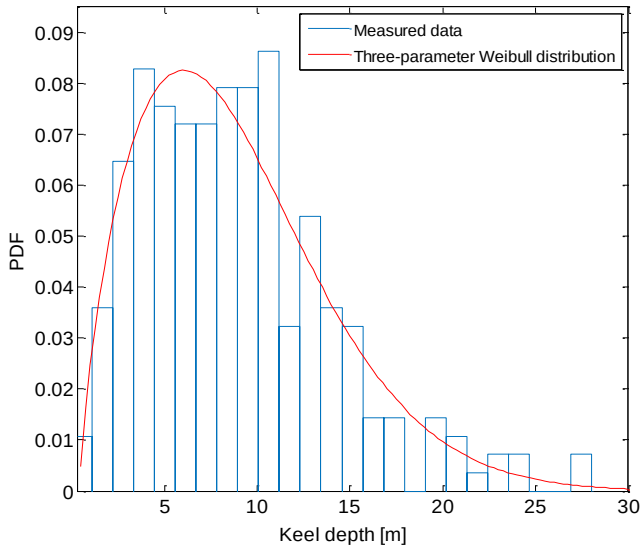

Figure 12. Probability density function for the keel draft h_k of first-year ice ridges in Arctic regions

Moreover, it should be mentioned that for the probabilistic description of the aforementioned key parameters of ice ridges, the seasonal effects have not been considered since relevant studies are limited and ongoing. Most of the aforementioned data sets were collected in the winter and spring seasons. For different phases of the first-year ice ridges and sea ice, which depend on the seasonal change, their morphological, physical and mechanical properties are quite different. Some recent progress for the seasonal effects can be found in Ervik et al. (2018), Shestov et al. (2018) and Wang et al. (2018).

5. Development of environmental contours

Based on the probabilistic models for the key parameters of ice ridges and the IFORM, different forms of environmental contours, such as two-dimensional contour lines, three-dimensional contour surface and four-dimensional manifold are developed in this Section. Application of the ECM for extreme ice loads estimation is only available and illustrated in Section 5.1, while prediction of ice loads for the models proposed in Sections 5.2 and 5.3 requires advanced numerical tool (or experiments) which is now under development within a joint project described in Hahn et al. (2017).

5.1 Two-dimensional contour lines

In this case, the ship and ice ridge interaction process is simplified as a slope structure that interacts with sheet ice and the structure induces flexural failure of the ice sheet. Then, the ice loads, F, acting on the ship structure can then be estimated by applying the empirical formula recommended by ISO (2010) or by a formula proposed in (Jordaan, 2001)

$$F = c_f \sigma_f h_{cl}^2 \tag{10}$$

where c_f is a parameter that accounts for the time-dependent flexural failure of ice and its value should be calibrated with full scale verification.

In this semi-analytical calculation, only the consolidated layer thickness, h_{cl} and the flexural strength of the ice feature σ_f are required. Obviously, such model is quite simple for evaluation of the ship and ice ridge interaction process since neither the ice crushing force nor the ridge keel actions have been considered. Nevertheless, this model can be applied as a basic case to illustrate the key steps for developing environmental contours as well as for application of the ECM to estimate of the extreme ice ridge loads. Furthermore, the influence of the correlation between the environmental parameters and the influence of the number of encountered ice ridge load events for a given return period, on the environmental contours can be easily studied due to the simplicity of two-dimensional environmental contours.

Since the distribution of the consolidated layer thickness depends on the geometrical location and we only have experimental data for h_{cl} that were collected in the Barents Sea in this work. It is assumed that the desired ice-capable ship mainly sails and operates in the Barents Sea with an annual voyage of 5000 km in the ice ridge field. The ice ridge density is 2/km along the route in this sea area (Arpiainen and Kiili, 2006). The service life of a desired icebreaker is assumed

to be 50 years and the number of ice ridges that will be encountered by the desired Arctic ship during its service life is determined as follows:

$$N_{50\,years} = 50 \cdot N_{1\,year} = 50 \cdot r \cdot 5000 \cdot 2 \tag{11}$$

where $N_{50years}$ and N_{1year} represent the number of ice ridges that will be encountered during the 50-year period and the 1-year period, respectively. In this work, it is assumed that for the 50-year period, the influence of global climate change on the ice conditions along the route is not considered. The annual number of ice ridges encountered by the ship is assumed to be a fixed value given as $N_{1year} = r \cdot 5000\text{km} \cdot 2/\text{km}$. r is the encounter frequency which depends on the experience of the crew and capability of the navigation equipment on board. Some ice ridges can be avoided during the voyage with assistance from the aforementioned two aspects, but currently, there has been no research work performed to determine the encounter frequency r. Moreover, many of what seems to be ridges from surface observations, produce very small or even no significant load for structures since these ridges may be young and have almost no consolidated layer.

For a 50-year return period, according to the IFORM, the radius of the circle in the U-space, β_F is determined as follow:

$$\beta_F = \Phi^{-1}(1 - p_f(y_N)) = \Phi^{-1}(1 - 1/N_{50\,years}) \tag{12}$$

The circle is plotted in Fig. 13 (a), u_1 and u_2 are independent standard Gaussian variables given by $u_1 = \beta_F \cdot \sin(\eta)$ and $u_2 = \beta_F \cdot \cos(\eta)$, respectively, in which the angle η varies from 0 to 2π. In this work, only the marginal PDFs of the environmental parameters are given, and the correlation between the key parameters is not available. Assume that the variables s_1 and s_2 represent the consolidated layer thickness and flexural strength of the ice features, respectively. The environmental contour in the physical parameter space can be obtained by the circle in the U-space with the application of the Nataf transformation given by Eq. 13:

$$\begin{aligned} s_1 &= F_{S_1}^{-1}(\Phi(u_1)) \\ s_2 &= F_{S_2}^{-1}(\Phi(u_2\sqrt{1-\rho_{12}'^2} + \rho_{12}'\Phi^{-1}(F_{S_1}(s_1)))) \end{aligned} \tag{13}$$

where ρ_{12} is the correlation coefficient between the consolidated layer thickness and flexural strength. The coefficient ρ'_{12} is the corresponding (equivalent) correlation coefficient used in the Nataf transformation, and its relationship with ρ_{12} can be approximated by a semi-empirical equation, which is given as follows:

$$\rho'_{12} = \zeta \cdot \rho_{12} \tag{14}$$

. Relevant descriptions for determining the function ζ can be found in Liu and Der Kiureghian (1986).

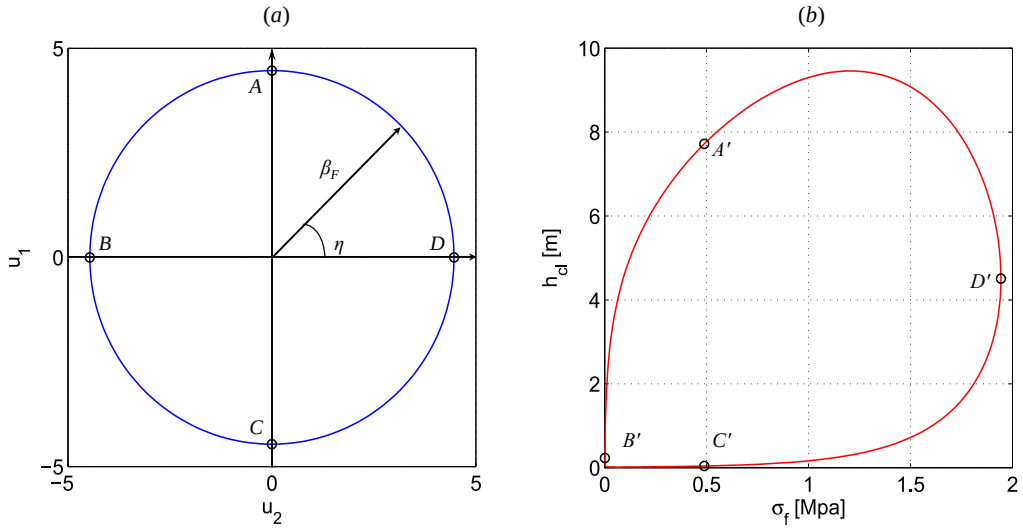

Figure 13. The circle in the U space with radius β_F (left) and the corresponding contour line in the physical parameter space (right)

In this case, both the correlation coefficient ρ_{12} and encounter frequency r are assumed to be 0.5. The corresponding contour line for a 50-year return period is presented in Fig. 13(b). In order to illustrate the Nataf transformation, four points denoted as A, B, C and D are selected on the circle in the U-space, then these points are mapped to the corresponding points denoted as A', B', C' and D' in the physical parameter space by applying the one-to-one mapping, i.e., the Nataf transformation.

After the generation of the contour line, the extreme load level, y_N, corresponding to a 50-year return period can then be estimated by the following relationship:

$$y_N \approx \max \text{loads for conditions along the } (s_1, s_2) \text{contour} \tag{15}$$

Assume that the parameter c_f is a fixed value, then estimation of the extreme loads is simplified as searching the most critical ice ridge condition along the contour line. The values of the correlation coefficient ρ_{12} and encounter frequency r are selected somewhat arbitrary due to the limitation of reference work. The influence of these two variable on the subsequent contour lines should be studied. Firstly, with a fixed value of 0.5 for r, the influence of the correlation coefficient ρ_{12} on the environmental contour is shown in Figure 14. The most critical ice ridge condition along each contour line is plotted as circle in this figure.

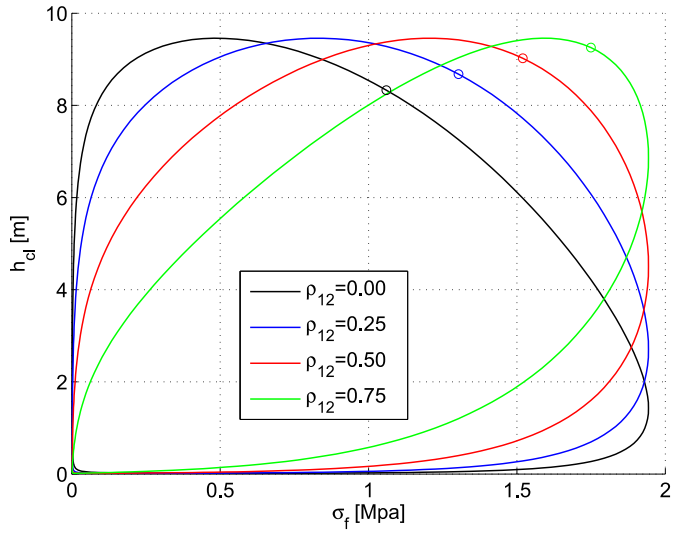

Figure 14. Influence of correlations between the consolidated layer thickness and flexural strength on the environmental contour lines associated with a 50-year return period, circles represent the most critical ice condition along the contour lines

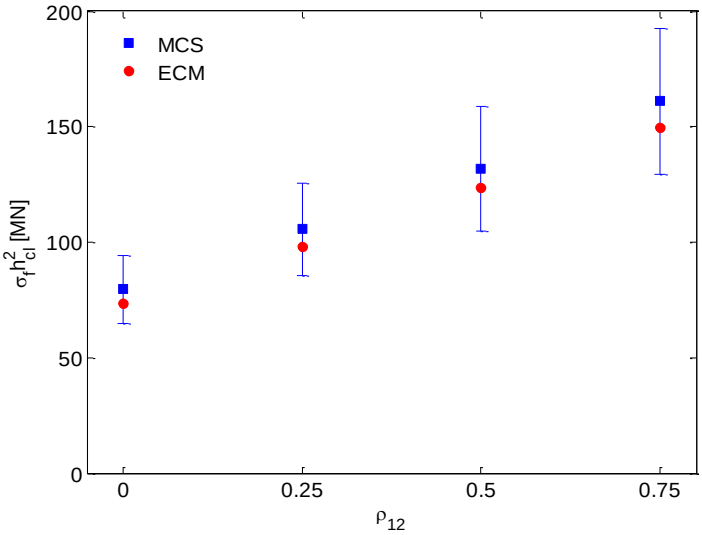

Figure 15. Estimation of the extreme ice loads associated with a 50-year return period by MCS and the ECM, the error bar indicates the standard deviation from the mean value

In order to evaluate the performance of the ECM, the straightforward MCS is applied in this work. For each case with a given value of correlation coefficient ρ_{12} and a fixed value of 0.5 for r, 100 sets of simulation are arranged to calculate the extreme ice load corresponds to a 50-year return period. There are 250000 realizations (i.e., $N_{50years}$) in each set of simulation. The extreme ice loads estimated by MCS and the ECM are shown in Fig 15. The straightforward MCS is a brute force technique to estimate the extreme values, it is seen that the results provided by MCS are suffered from large uncertainties. Moreover, for each case with 100 sets of simulation the computation time is more than 1 hour on a personnel computer, even though the ice load for

such simple model can be provided by the semi-analytical formula (10). For the ECM, it is seen that the predicted extreme ice loads are very close to the MCS results, but with significant less computation burden. Therefore, the ECM can serve as an effective way to estimate the extreme ice loads.

As shown in Fig. 14, the variation of the correlation coefficient has a quite important effect on the shapes of the enviromental contour lines. The critical region with large values of the consolidated layer thickness and flexural strength becomes narrow as the correlation coefficient increase. A narrower critical region implies that large values of the consolidated layer thickness are more easily (or more probably) accompanied by large values of the flexural strength, which would cause more serious ice loads. It is seen in Figs 14 and 15, with the increment of the correlation coefficient, the maximum loads for the ice conditions along the contour line, as well as the extreme load level associated with 50-year return period increase. Moreover, it is seen in Fig. 14 that the most serious ice conditions on environmental contour lines with a 50-year return period usually have large values of $h_{cl.}$ In fact, for relative thick ice, only a bending failure mode to determine the ice loads is not enough, more reliable models should be introduced to study the ship and ice ridge interaction process.

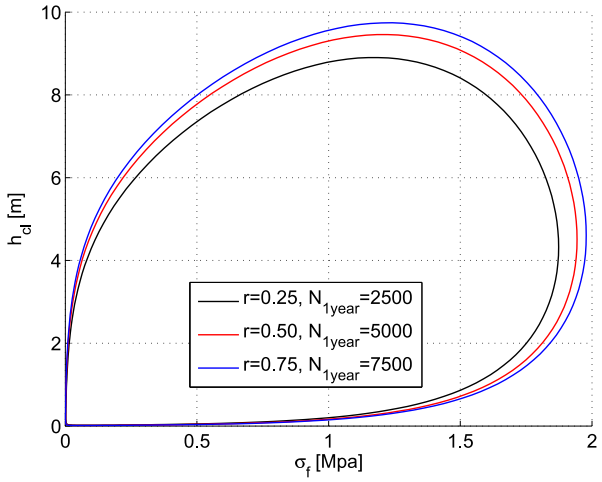

Figure 16. Environmental contour lines for various values of the encounter frequency r (ρ_{12}=0.50)

Then, the influence of the encounter frequency r on the environmental contour is studied by keeping the correlation coefficient as a fixed value of 0.50. The contour lines for different values of r are plotted in Fig. 16. The contour lines have similar shapes due to having the same value of the correlation coefficient. An increased value of r implies that more load events will be

encountered by the Arctic ship for the same return period. Moreover, the contour lines have broader ranges for the same return period as the encounter frequency increases, since the radius β_F given by Eq. 12 increases with the number $N_{50years}$ which is expressed as Eq. 11. Obviously, it is seen in Fig. 16 that with the increment of r, the corresponding maximum loads for the ice ridge condtions along the contour line and the extreme load level, y_N increase.

Furthermore, it is shown that the number of ice ridge load events encountered by an Arctic ship for a given return period has a significant influence on the environmental contour. This number is dependent on the encounter frequency r, length of annual voyage and ice ridge density along the route in the ice ridge fields. For the reliability-based design of Arctic ships, a proper consideration of these aspects is required.

5.2 Three-dimensional contour surface

In order to obtain more reliable results, a model with three key parameters of the ice ridges is proposed in this section. The main loads for the ship and ridge interaction are assumed to be dominated by the consolidated layer part and the effect from unconsolidated rubbles is still not considered. In this model, the dynamic effects of the ship and ice interaction process are considered. Therefore, the consolidated layer thickness, flexural strength and crushing strength of the ice features should be considered and numerical simulations are required to calculate the ice ridge loads. Assume that the variable s_3 represents the crushing strength of the ice feature and the variable u_3 denotes its corresponding transformed value in the U-space according to the Nataf model given by Eq. 16 for the three-dimensional transformation:

$$
\begin{aligned}
s_1 &= F_{S_1}^{-1}(\Phi(u_1)) \\
s_2 &= F_{S_2}^{-1}(\Phi(u_2\sqrt{1-\rho_{12}'^2} + \rho_{12}'\Phi^{-1}(F_{S_1}(s_1)))) \\
s_3 &= F_{S_3}^{-1}(\Phi(\frac{u_3}{\sqrt{1-\rho_{12}'^2}}\sqrt{1-\rho_{12}'^2-\rho_{13}'^2-\rho_{23}'^2+2\rho_{12}'\rho_{13}'\rho_{23}'} \\
&\quad + \frac{1}{1-\rho_{12}'^2}((\rho_{13}'-\rho_{12}'\rho_{23}')\Phi^{-1}(F_{S_1}(s_1)) + (\rho_{23}'-\rho_{12}'\rho_{13}')\Phi^{-1}(F_{S_2}(s_2))))
\end{aligned}
\tag{16}
$$

where the coefficients ρ'_{ij} (i, j =1, 2, 3; $i \neq j$) are the equivalent correlation coefficients used in the Nataf transformation.

In this case, it is assumed that the correlation coefficients between the three parameters included in this model equal 0.5. The encounter frequency r is assumed to be 0.5 and other parameters are set the same as the values given in Section 5.1. Similar to the two-dimensional

environmental contours obtained by the IFORM, a three-dimensional sphere with radius β_F, given by Eq. 12, is created in the *U*-space. Then, the sphere is transformed into a three-dimensional environmental contour surface according to the Nataf model described by Eq. 16. The 50-year environmental contour surface with three key parameters., i.e. the consolidated layer thickness, flexural strength and crushing strength of ice features is plotted in Fig. 17.

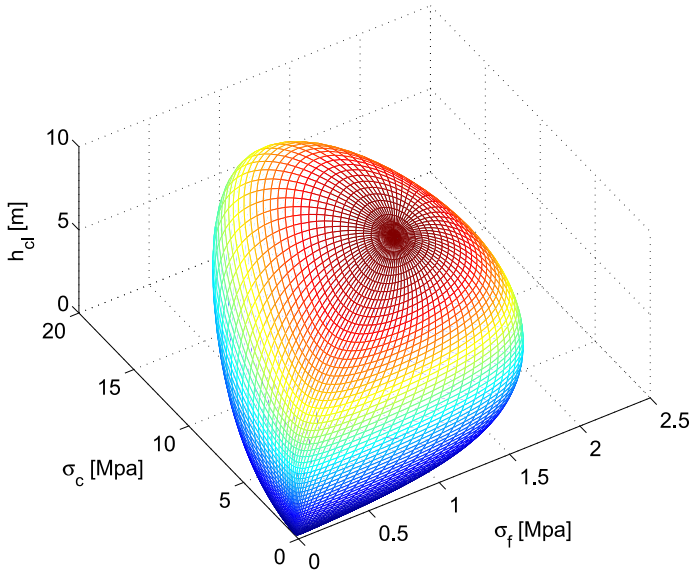

Figure 17. The 50-year contour surface for the consolidated layer thickness, flexural strength and crushing strength

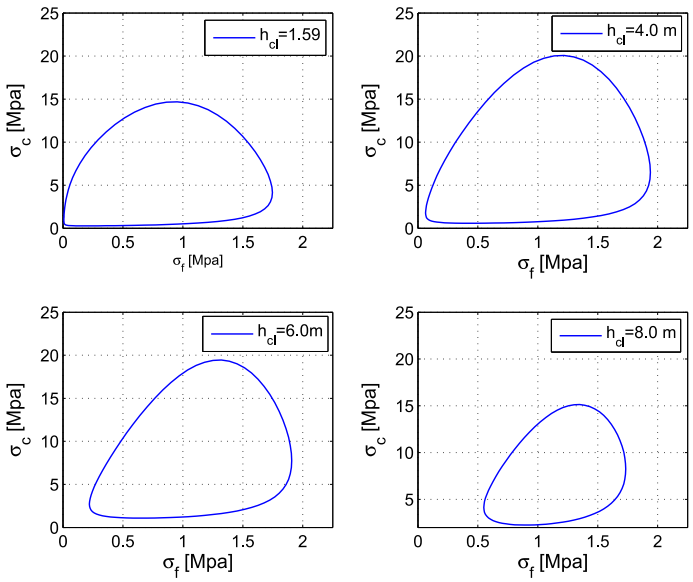

Figure 18. Two-dimensional contour lines on the 50-year contour surface for different values of the consolidated layer thickness

Moreover, in order to present a detailed view of the contour surface, the two-dimensional contour lines on the 50-year environmental contour for different values of the consolidated layer thickness are plotted in Fig. 18. In these selected consolidated layer thicknesses, h_{cl} = 1.59 m is the mean value of the Gamma distribution given by Eq. 5. Similar to the two-dimensional contour lines, after establishing enviromental contour surfaces with three key parameters, limited ice ridge conditions with fixed values of key parameters are selected on contour surfaces for numerical calculation or experiments. The most serious ice ridge conditions are searched and used to estimate the extreme ice ridge loads corresponding to a 50-year return period.

5.3 Four-dimensional contour manifold

As a futher development of the abovementioned models, a more realistic model is proposed in this Section. In this model, both the dynamic effects of the consolidated layer part and ship structure interaction as well as the loads effect from the rubble blocks can be considered, which means all of the four key parameters are considered in the model.

As mentioned in the ISO (2010) standard, existing field data suggest that the keel draft h_k and consolidated layer thickness h_{cl} are not correlated with each other. In addition to this suggestion, it is assumed that there is no correlation between h_k and the ice strength σ_f and σ_c. Assume that s_4 represents the keel draft and u_4 denotes the corresponding value in the U-space. For a given value of the keel draft, the corresponding value u_4 is obtained by applying the transformation given by Eq. 17.

$$s_4 = F_{S_4}^{-1}(\Phi(u_4)) \tag{17}$$

The correlation coeffients ρ_{ij} (i, j =1, 2, 3; $i \neq j$) are set as 0.5, the encounter frequency r =0.5 and the other parameters are kept the same as those given in Section 5.1. In order to visualize the 50-year environmental contour with four parameters, which is formed as a manifold, environmental contour surfaces with different values of the keel draft are presented in Fig. 19. Specifically, for a given value of the keel draft, the contour surface is obtained by transforming the sphere in the U-space with the radius β_F' calculated using the following equation:

$$\beta_F' = \sqrt{\beta_F^2 - u_4^2} \tag{18}$$

into the physical parameter space with the Nataf model given by Eq. 16.

It is seen that the contour surfaces for different values of h_k have similar shapes due to having the same correlation relationships between the four key parameters. For keel drafts higher than

the mean value (h_k = 8.89 m), the volume covered by the contour surface decreases as the keel drafts increase because the radius β'_F for the sphere in the U-space decreases as the value of u_4 increases when u_4>0. After the establishment of the contour manifold for the 50-year return period, the next step is to find the most serious ice ridge conditions located on the manifold, by applying numerical simulation or experiment, to estimate the extreme ice ridge loads acting on the Arctic ship.

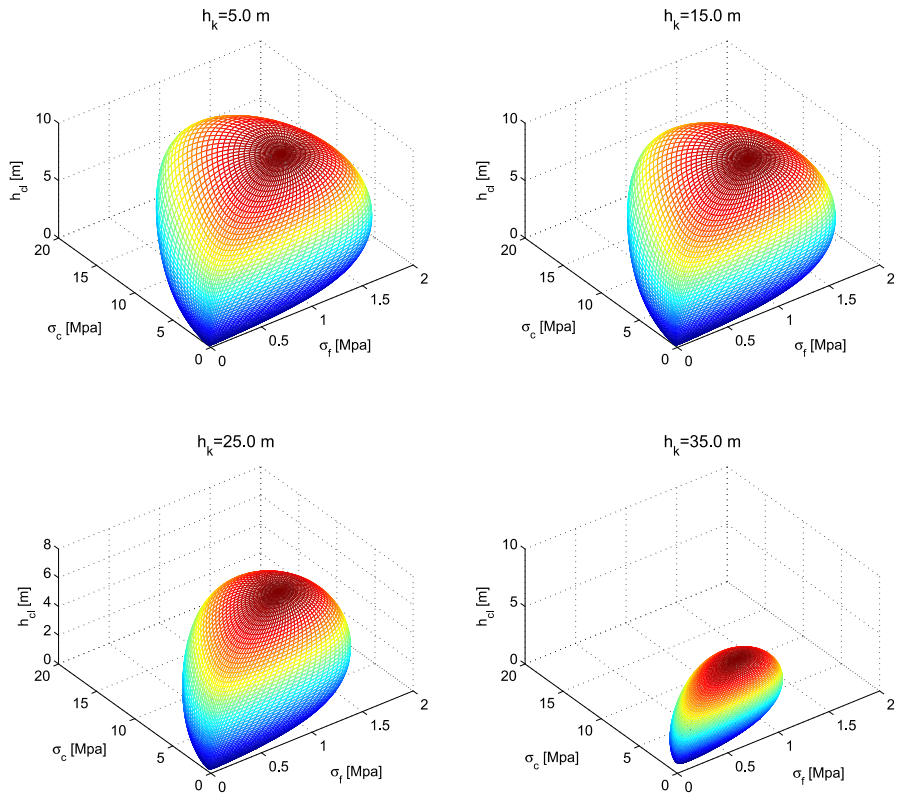

Figure 19. Three-dimensional contour surfaces from the 50-year contour manifold for different values of keel draft h_k

Based on the environmental contours developed in this section, it is seen that more realistic model for studying the ship and ice ridge interaction process requires more kinds of key parameters and then increases the dimension of environmental contour. From this point of view, environmental contours with higher dimensions are more reliable to estimate the extreme ice ridge loads. However, the computation burden for each simulation case would be higher for more realistic model and the straightforward MCS used to estimate the extreme ice loads would be formidable. Searching the most serious ice ridge conditions located on the contour to estimate the extreme loads would be more attractive and practical.

6. Conclusions

In this work, based on the ship and ice ridge interaction process, four parameters of the first-year sea ice ridge are identified as the key parameters for determining the ice ridge loads on a ship hull. Probabilistic models are applied to describe the collected data for the key parameters. The principle of the environmental contour method used for reliability-based design of Arctic ships is illustrated. By applying the IFORM, different forms of environmental contours are generated according to different simplifications introduced for the ship and ice ridge interaction process.

The influence of the correlation between the environmental parameters and encounter frequency r on the environmental contour has been studied. It is recommended that additional research work should be performed to study the correlation between the physical and mechanical parameters of first-year sea ice since the correlation relationship has an important effect on the environmental contour as well as on the extreme load acting on the ship hull.

Furthermore, the number of ice ridge load events encountered by an Arctic ship for a given return period is also important for the reliability-based design. This number depends on the encounter frequency r, distance of the annual voyage and ice ridge densities along the sailing route in different ice ridge fields. Additionally, global climate change also has a potential influence on the ice ridge density and properties of ice ridges. A detailed study of these factors could promote the development of the proposed environment contour method.

The current work only considers the data of the consolidated layer thickness collected in the Barents Sea. The distributions of the surrounding level ice thickness and consolidated layer thickness for first-year sea ice ridges in other sea areas along Arctic shipping routes are under development. Establishment of environmental contours that cover different sea ice regions will be performed in a future study.

Acknowledgments

The authors would like to thank the Lloyd's Register Foundation for funding the Joint Center of Excellence for Arctic Shipping and Operations (project number: 650263) which enabled this work. Lloyd’s Register Foundation helps to protect life and property by supporting engineering-related education, public engagement and the application of research. Financial support from the Research Council of Norway (RCN project number: 249272/O80) is also acknowledged.

References

Arpiainen, M., Kiili, R., 2006. Arctic shuttle container link from Alaska US to Europe, Helsinki: Aker Arctic Technology (Report k-63).

Bonath, V., Patil, A., Fransson, L., Sand, B., 2013. Laboratory testing of compressive and tensile strength on level ice and ridged ice from Svalbard region, International Conference on Port and Ocean Engineering under Arctic Conditions.

Chai, W., Leira, B.J., 2018. Environmental contours based on inverse SORM. Marine Structures 60, 34-51.

Chai, W., Leira, B.J., Naess, A., 2018. Probabilistic methods for estimation of the extreme value statistics of ship ice loads. Cold Regions Science and Technology 146, 87-97.

Dalane, O., Aksnes, V., Løset, S., 2015. A Moored Arctic Floater in First-Year Sea Ice Ridges. Journal of Offshore Mechanics and Arctic Engineering 137 (1), 011501.

DNV.GL, 2017. Enviromental Conditions and Enviromental Loads (DNV-RP-C205). Det Norske Veritas AS, Oslo.

Eckert-Gallup, A.C., Sallaberry, C.J., Dallman, A.R., Neary, V.S., 2016. Application of principal component analysis (PCA) and improved joint probability distributions to the inverse first-order reliability method (I-FORM) for predicting extreme sea states. Ocean Engineering 112, 307-319.

Ehlers, S., Cheng, F., Jordaan, I., Kuehnlein, W., Kujala, P., Luo, Y., Freeman, R., Riska, K., Sirkar, J., Oh, Y.-T., 2017. Towards mission-based structural design for arctic regions. Ship Technology Research 64 (3), 115-128.

Ervik, Å., Høyland, K.V., Shestov, A., Nord, T.S., 2018. On the decay of first-year ice ridges: Measurements and evolution of rubble macroporosity, ridge drilling resistance and consolidated layer strength. Cold Regions Science and Technology 151, 196-207.

Gong, H., Polojärvi, A., Tuhkuri, J., 2017. Preliminary 3D DEM Simulations on Ridge Keel Resistance on Ships. POAC.

Hahn, M., Dankowski, H., Ehlers, S., Erceg, S., Rung, T., Huisman, M., Sjöblom, H., Leira, B.J., Chai, W., 2017. Numerical Prediction of Ship-Ice Interaction: A Project Presentation, ASME 2017 36th International Conference on Ocean, Offshore and Arctic Engineering. American Society of Mechanical Engineers, p. V008T007A002.

Haver, S., Winterstein, S.R., 2009. Environmental contour lines: A method for estimating long term extremes by a short term analysis. Transactions of the Society of Naval Architects and Marine Engineers 116, 116-127.

Høyland, K.V., 2014. Ice ridge characteristics and engineering concerns regarding ice ridges, Proceedings of the 22nd IAHR International Symposium on Ice, Singapore.

Huisman, M., Janßen, C.F., Rung, T., Ehlers, S., 2016. Numerical simulation of ship-ice interactions with physics engines under consideration of ice breaking, The 26th International Ocean and Polar Engineering Conference. International Society of Offshore and Polar Engineers.

Huseby, A.B., Vanem, E., Natvig, B., 2013. A new approach to environmental contours for ocean engineering applications based on direct Monte Carlo simulations. Ocean Engineering 60, 124-135.

ISO, 2010. 19906: Petroleum and Natural Gas Industries–Arctic offshore structures. Geneva: ISO.

Jordaan, I.J., 2001. Mechanics of ice–structure interaction. Engineering Fracture Mechanics 68 (17-18), 1923-1960.

Kujula, P., 1994. On the statistics of ice loads on ship hull in the Baltic. Helsinki University of Technology.

Kuuliala, L., Kujala, P., Suominen, M., Montewka, J., 2017. Estimating operability of ships in ridged ice fields. Cold Regions Science and Technology 135, 51-61.

Leira, B.J., 2008. A comparison of stochastic process models for definition of design contours. Structural Safety 30 (6), 493-505.

Lemee, E., Brown, T., 2005. Review of ridge failure against the confederation bridge. Cold Regions Science and Technology 42 (1), 1-15.

Lensu, M., 2002. Short term prediction of ice loads experienced by ice going ships. Helsinki University of Technology.

Liu, P.-L., Der Kiureghian, A., 1986. Multivariate distribution models with prescribed marginals and covariances. Probabilistic Engineering Mechanics 1 (2), 105-112.
Lu, W., Lubbad, R., Løset, S., 2014. Simulating ice-sloping structure interactions with the cohesive element method. Journal of Offshore Mechanics and Arctic Engineering 136 (3), 031501.
Madsen, H.O., Krenk, S., Lind, N.C., 2006. Methods of structural safety. Courier Corporation.
Myland, D., 2014. Ships Breaking Through Sea Ice Ridges. International Journal of Offshore and Polar Engineering 24 (01), 28-34.
Ranta, J., Polojärvi, A., Tuhkuri, J., 2018. Ice loads on inclined marine structures-Virtual experiments on ice failure process evolution. Marine Structures 57, 72-86.
Riska, K., 1987. On the mechanics of the ramming interaction between a ship and a massive ice floe. Publications Valtion Teknillien Tutkimuskeskus (43).
Riska, K., Bridges, R., 2017. Limit state design and methodologies in ice class rules for ships and standards for Arctic offshore structures. Marine Structures.
Rosenblatt, M., 1952. Remarks on a multivariate transformation. The annals of mathematical statistics 23 (3), 470-472.
Sand, B., Horrigmoe, G., 2001. Simulations of ice ridge forces on conical structures, The Eleventh International Offshore and Polar Engineering Conference. International Society of Offshore and Polar Engineers.
Sanderson, T.J., 1988. Ice mechanics and risks to offshore structures. Springer.
Shestov, A., Høyland, K., Ervik, Å., 2018. Decay phase thermodynamics of ice ridges in the Arctic Ocean. Cold Regions Science and Technology 152, 23-34.
Silva-González, F., Heredia-Zavoni, E., Montes-Iturrizaga, R., 2013. Development of environmental contours using Nataf distribution model. Ocean Engineering 58, 27-34.
Strub-Klein, L., 2017. A Statistical Analysis of First-Year Level Ice Uniaxial Compressive Strength in the Svalbard Area. Journal of Offshore Mechanics and Arctic Engineering 139 (1), 011503.
Strub-Klein, L., Sudom, D., 2012. A comprehensive analysis of the morphology of first-year sea ice ridges. Cold Regions Science and Technology 82, 94-109.
Su, B., Riska, K., Moan, T., 2010. A numerical method for the prediction of ship performance in level ice. Cold Regions Science and Technology 60 (3), 177-188.
Sudom, D., Timco, G., 2013. Knowledge gaps in sea ice ridge properties.
Tan, X., Su, B., Riska, K., Moan, T., 2013. A six-degrees-of-freedom numerical model for level ice–ship interaction. Cold Regions Science and Technology 92, 1-16.
Timco, G., O'Brien, S., 1994. Flexural strength equation for sea ice. Cold Regions Science and Technology 22 (3), 285-298.
Timco, G., Weeks, W., 2010. A review of the engineering properties of sea ice. Cold Regions Science and Technology 60 (2), 107-129.
Vanem, E., 2017. A comparison study on the estimation of extreme structural response from different environmental contour methods. Marine Structures 56, 137-162.
Wadhams, P., 1980. A comparison of sonar and laser profiles along corresponding tracks in the Arctic Ocean. Sea ice processes and models, 283-299.
Wang, Q., Li, Z., Lei, R., Lu, P., Han, H., 2018. Estimation of the uniaxial compressive strength of Arctic sea ice during melt season. Cold Regions Science and Technology 151, 9-18.
Wikipedia, edited on May 4, 2018. https://en.wikipedia.org/wiki/Arktika-class_icebreaker.
Winterstein, S.R., Ude, T.C., Cornell, C.A., Bjerager, P., Haver, S., 1993. Environmental parameters for extreme response: Inverse FORM with omission factors. Proceedings of the ICOSSAR-93, Innsbruck, Austria, 551-557.